Monitoring diesel engine parameters based on FBG probe*

ZHANG Hao (张豪), **JIANG Qi** (蒋奇)**, **WANG Bao-yan** (王保岩), **and WANG Jun-jie** (王俊杰)
School of Control Science and Engineering, Shandong University, Jinan 250061, China

(Received 18 July 2016)

This paper proposes an unprecedented systematic approach for real-time monitoring the temperature and flow of diesel engine by using embedded fiber Bragg grating (FBG). By virtue of FBG's temperature effect, we design a novel sensitive FBG temperature sensing probe to measure the temperature of cylinder head and inlet flow of diesel engine. We also establish the corresponding software platform for intuitive data analysis. The experimental and complementary simulation results simultaneously demonstrate that the FBG-based optical fiber technique possesses extraordinary reproducibility and sensitivity, which makes it feasible to monitor the temperature and inlet flow of diesel engine. Our work can provide an effective way to evaluate the thermal load of cylinder head in diesel engine.
Document code: A **Article ID:** 1673-1905(2016)05-0384-5
DOI 10.1007/s11801-016-6162-7

The cylinder head is one of the most fragile parts among all the components of the diesel engine. During the working process, the temperature gradient produced on the cylinder head perhaps leads to large thermal stress which can break the cylinder head and shut down the engine. Therefore, a real-time thermal monitor is critical to analyse the stress caused by thermal imbalance on the cylinder head. Until now, traditional electrical sensors, such as thermocouple and thermal resistance, were applied in the temperature test on the cylinder head[1-3], which are insufficient to the engineering requirements, such as slow thermocouple response, vulnerability to electromagnetic interference (EMI) and poor dynamic performance. In addition, the installation of traditional electrical sensors is inconvenient and unprecise when performing the test on the cylinder head, which further increases its measurement errors.

Optical fiber sensor possesses prominent advantages than the traditional electrical sensors. Except for the tolerance to severe environment like high temperature and significant anti-EMI properties, optical fiber sensor with simple structure can be easily installed on the target. The fiber Bragg grating (FBG) temperature sensor has been paid more attentions in the field of high temperature measurement of engine. Joseba et al[4] investigated a new approach for monitoring tip clearance and tip timing in aircraft engines at low cost and high resolution based on a reflective, intensity-modulated optical fiber sensor. Yang et al[5] launched a research for measuring strain of interfacial bonding layer in solid rocket engine under after-cure cooling by designing a optical fiber sensor based on flush type. Fan et al[6] designed an optical fiber probe based on distributed fiber-optic sensor for engine temperature monitoring. A new optical fiber tip-timing sensor which can resist 650 °C high temperature was designed[7] to meet the high temperature requirements for the vibration monitoring of aero-engine compressor blades. Meanwhile, a novel method for online monitoring engine oil quality based on tapered optical fiber sensor was proposed[8] with a highly sensitive and rapidly respond. However, the development of optical fiber sensor on diesel engine has not been reported before.

By taking advantages of FBG sensor, we obtain the temperature distribution on the cylinder head and inlet flow measurement of diesel engine. The optimal sensor structure is proposed and produced to accommodate the test environment. In addition, temperature field simulation is performed by the coupling simulation method. We also develop a real-time monitoring system based on J2EE architecture. Finally, the temperature test and an inlet flow simulation on the cylinder head are designed and implemented to verify the theoretical analysis. The performance parameters, such as linearity, sensitivity and repeatability, are obtained from our experiments.

According to the fiber coupled mode theory[6,9-11], periodic distribution of refractive index of optical fiber is characterized as an equivalent filter. When the light including a plurality of wavelength signals passing through the grating, broadband light can generate mode coupling, and the light that satisfies the Bragg condition is re-

* This work has been supported by the National Natural Science Foundation of China (Nos.61271073 and 61473175), and the Fundamental Research Funds of Shandong University (No.2015JC040).
** E-mail: jiangqi@sdu.edu.cn

flected. The Bragg condition is expressed as

$$\lambda_B=2n_{eff}\Lambda, \tag{1}$$

where λ_B is the center wavelength of FBG, n_{eff} is the effective refractive index of fiber core, and Λ is the period of grating.

Temperature and strain changes directly lead to the offset of center wavelength. When the temperature changes, the fiber grating generates thermo-optic effect, thermal expansion effect and elastic-optic effect. These reactions can impact on the grating period and the refractive index, and then resulting in the change of the center wavelength of the reflected wave. After eliminating the waveguide effect, the FBG temperature response has the following characteristics:

$$\frac{d\lambda_B}{dT}=2\left(n_{eff}\frac{d\Lambda}{dT}+\Lambda\frac{dn_{eff}}{dT}\right)=(\alpha+\zeta)\lambda_B, \tag{2}$$

where $\alpha=\frac{1}{\Lambda}\frac{d\Lambda}{dT}$ and $\zeta=\frac{1}{n_{eff}}\frac{dn_{eff}}{dT}$ are thermal expansion coefficient and thermo-optic coefficient of the FBG, respectively. Simply, we propose the temperature sensitivity coefficient $K_T=(\alpha+\zeta)$, and then Eq.(2) can be simplified as

$$\frac{\Delta\lambda_{BT}}{\lambda_{BT}}=(\alpha+\zeta)\Delta T=K_T\Delta T, \tag{3}$$

which demonstrates that the wavelength shift of FBG is proportional with temperature. So the temperature change can be obtained directly by measuring the wavelength shift of FBG.

In order to cope with the high temperature environment, FBG should be coated by the polyimide, which makes it resistant to high temperature up to 350 °C[12]. To obtain the FBG wavelength-temperature curve, the calibration of the FBG sensors in the standard ambient temperature is required before packaging. By taking into account the measurement accuracy, the calibration is divided into two sections, in the water tank for the low temperature calibration and in the oven for the high temperature calibration.

The calibration of the FBG sensors was first conducted in a water thermostat system with the error less than ±0.01 °C. We tracked the temperature of water thermostat and grating wavelengths every 10 °C when the temperature changed from 20 °C to 90 °C in the water tank. The calibration of the FBG sensors in high temperature was performed from 30 °C to 380 °C in the oven. The temperature of oven and the grating wavelength values were recorded every 30 °C. Finally, the full FBG temperature wavelength curves can be achieved as shown in Fig.1[13,14]. Based on the calibration results, the temperature linearity for individual FBG is obtained as 0.999 4 accompanying with the temperature sensitivity of 0.012 6 nm /°C.

It's necessary to fully package the FBG sensor before install it on the cylinder head as it's fragile and sensitive to the external strain. The conventional packaging schemes are surface mount type or tube type[15]. However the linear expansion of grating is not uniformly distributed in surface mount type, and there are sensitivity hysteresis and linearity decrease in tube type[16]. Here, we propose a novel type of sensor based on the metal tube package with the schematic structure shown in Fig.2. FBG was unfixed at the end of the metal tube. The transmission fiber was protected by yellow casing excluding the part where the transmission fiber was encircled by metal tube. The external diameter for the metal tube is 1 mm with wall thickness of 0.1 mm. The other end of metal tube was joined with yellow casing by using high-temperature resisting glue.

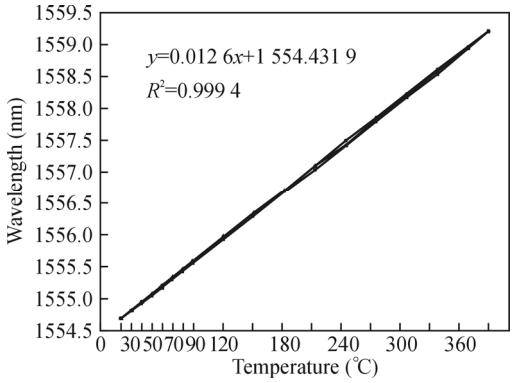

Fig.1 Wavelength versus temperature of FBG

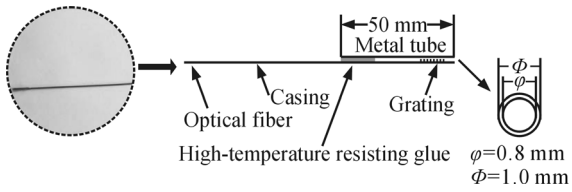

Fig.2 Schematic diagram of structure and material components of probe

Before the experiment, the temperature field simulation was conducted by using coupled simulation method and a fluid-structure interaction module in ANSYS[14]. The temperature field distribution on the cylinder head is shown in Fig.3. The heat energy expands from the fire deck to the outer surface. The highest temperature area in the engine wall locates in the exhaust side near the injector fitting hole and bridge zone. And the maximum temperature area of combustion surface appears in the bridge zone close to exhaust side due to the heating from the combustion of high temperature gas mixture. The highest temperature is over 600 °C. The wall temperatures near the water inlet port and the gas inlet port of approximately 140—280 °C are smaller compared with that of the combustion surface owing to the fluid cooling near this area. The exhaust side is affected by the action of high temperature heat transferring from combustion surface, and the temperature in this area ranges approximately from 190 °C to 340 °C.

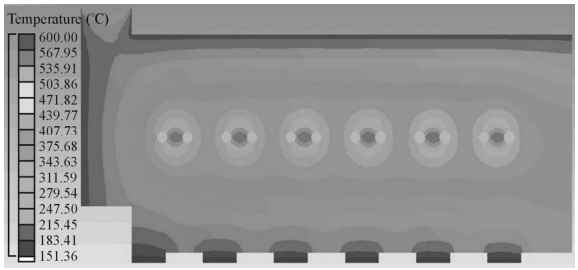

Fig.3 The temperature field distribution of the cylinder head

The experiments were conducted on Dongfeng Motor Corporation X7 diesel engine. Four cylinder heads were chosen and labelled as No.1—No.4, respectively. Here we mainly focused on Nos.2 and 3 cylinder heads, where the thirty measuring points were selected as shown in Fig.4. Each location had a hole with a diameter of 20.1 mm and distinctive depth. These points were divided into 15 groups, and each group was consisted of two points in the same depth but keeping the distance (3 mm) away from one another in the vertical direction. 7 groups were categorized into inlet side, while 7 groups were categorized into in exhaust side, and the remaining group was in the row of the cylinder. The FBG probe should be customized to prevent the damage of FBG resulting from the different depths of holes. Different installation strategies should be taken to avoid breaching the FBG sensor in the inlet valve and the exhaust valve of the cylinder head.

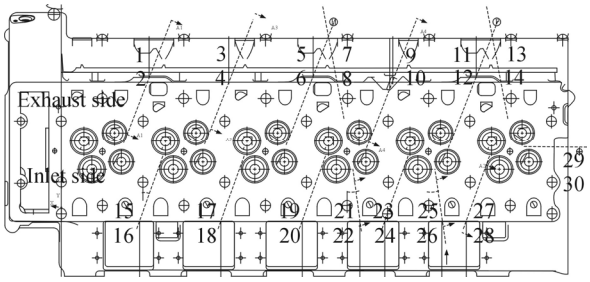

Fig.4 Distribution of measuring points on Nos.2 and 3 cylinder heads

Fig.5 shows photos with the probes installed in the inlet side and the exhaust side of the cylinder head. It should be addressed that in order to simplify procedures, the sensor in inlet side has to be installed before configuring cylinder head. We firstly removed the fan-shaped area around the mounting hole and exposed the mounting hole to the air. Secondly, we carefully inserted the FBG sensor into the hole before reaching the bottom and fixed it on the lower wall with glue. After 4 h, the former sector area was affixed onto the inlet pipe by sealant. Finally, we placed cylinder head armed with sensor probe back to the diesel engine.

It's also necessary to insulate the probe as the temperature of the exhaust pipe is more than 600 °C when the diesel engine works, which exceeds to the limit to the casing of optical fiber (200 °C). At first, we installed a metal baffle between the exhaust port and the mounting hole. Meanwhile, the fire blanket with bilayer fiberglass twills was set up between the baffle and the air vent. Then, we sheathed optical fiber ferrule with fireproof casing woven by non-alkali fiberglass, and kept two close probes into the same fiber casing. Fireproof casing only protected yellow tube and the probe part with metal case kept being exposed. The procedure of installation of the probe was similar to that on the inlet side. The different point was that a fire blanket made of heat-resisting fiberglass was used to enwrap the fireproof casing, and a piece of metal wire was employed to attach the optical fiber sensors to the engine bench.

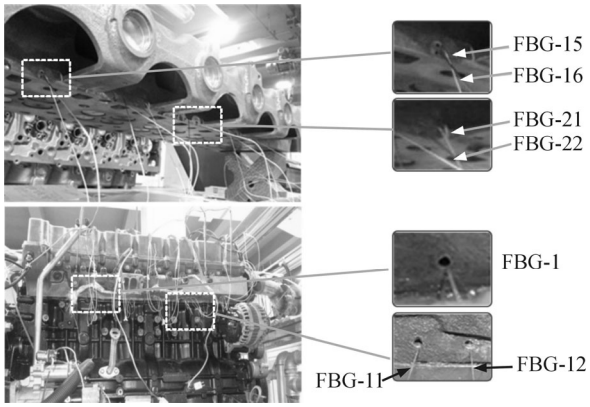

Fig.5 The installation of probe in the inlet side and the exhaust side of the cylinder head

We develop a software to monitor multiple channel of temperature signal with fiber optic sensor. As shown in Fig.6, the current software system adopts the J2EE architecture based on the combination of Flex, LCDS, EJB3.0 and Servlet functions, which can be divided into two sections of Flex server and Java client.

In our experiment, the real-time temperature signals in 16 channels can be collected directly with our software. We use the platform to record the temperatures of inlet and exhaust of diesel engine during the whole working process with the following procedure. ①The engine works 3—5 min in idle condition. ②Speed the engine up to 1 200 r/min and torque of 300 N·m, and hold them for 5 min. ③Speed the engine up to 1 500 r/min and torque of 500 N·m, and keep them for 5 min. ④Speed the engine up to 1 900 r/min and torque of 800 N·m, and keep them for 5 min equally. ⑤Speed the engine up to the rated power of 2 300 r/min and 1 050 N·m. ⑥Switch the engine to idle speed dramatically and stop the engine after 3—5 min.

As the diesel engine parameters keep constant in rated condition, the measured temperature in rated power remains stable with a margin of error of 3 °C. As shown in Fig.7, the measured values in inlet side are approximately 190—340 °C, and the range of measured values in exhaust side varies from 200 °C to 320 °C. The temperature on cylinder row (FBG-30) is higher than

those at other locations and reaches up to 370 °C. The temperatures of lower measuring points which are close to the combustion chamber are higher (70—150 °C) than those of the measuring points in the same group. The results from our experiments agree pretty well with the previous thermal field simulation.

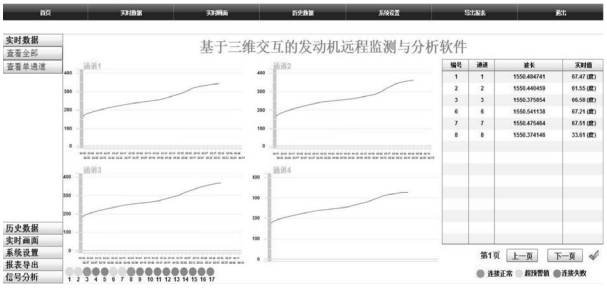

Fig.6 Schematic interface of the real-time temperature monitoring software

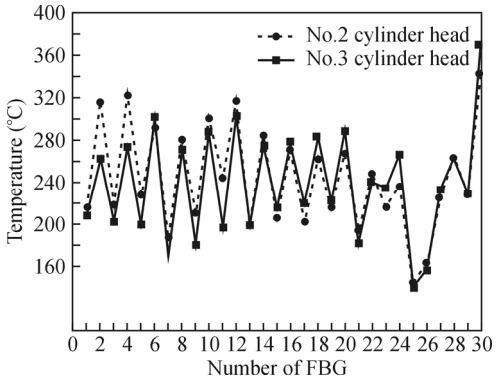

Fig.7 Temperature analysis of different measuring points on Nos.2 and 3 cylinder heads

To ensure the accuracy of the measurements, repetitive tests were performed in five measurement points of 11, 12, 13, 29 and 30 (as shown in Fig.4) on the No.3 cylinder head, respectively. We speeded the engine up to 2 300 r/min at rated condition, and then gradually reduced the speed to 800 r/min by decreasing 100 r/min or 200 r/min once. Finally, 11 sets of temperature signals were collected and analyzed. Fig.8 shows the evolution of temperature in five different measuring points under different working conditions. The temperature curves have the similar decreasing trend for all kinds of working conditions, which reveals that the experiment is repeatable and scalable with the optical sensor.

Fig.9 depicts a comparison of test data of the repetitive experiment and the first experiment on No.3 cylinder under the working conditions. 11 and 12 or 29 and 30 are the adjacent points in the same measurement group. As shown in Fig.9, large temperature differences are observed in the adjacent points. For the first experiment and the repetitive experiment, the temperature differences between 29 and 30 are 142.22 °C and 145.73 °C, while those between 11 and 12 are 107.08 °C and 55.92 °C, respectively. The temperatures in measurement points of 13, 29 and 30 in repetitive experiments are lower than that from the first experiment as approximately 10 °C, while the temperature differences are much larger in 11 and 12. The discrepancies can be attributed to that the hydraulic pressure during the repetitive experiments is lower than the normal value, which probably leads to abnormality in the temperature test.

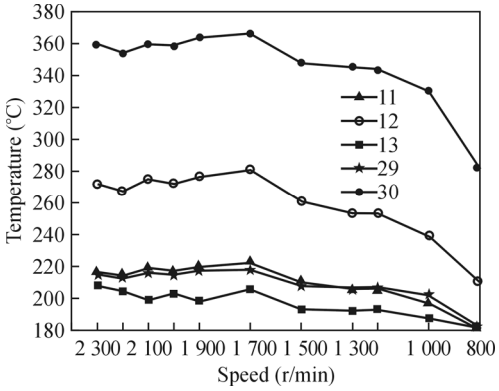

Fig.8 Temperature evolution in five different measuring points on No.3 cylinder head

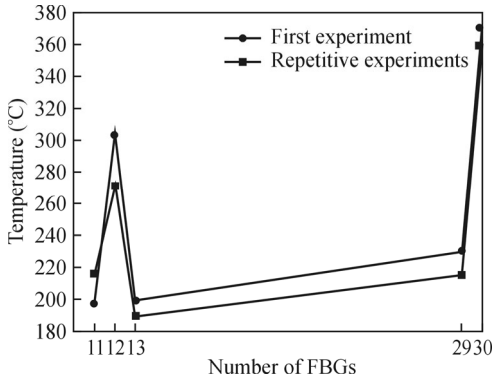

Fig.9 Temperature test data comparison between repeated experiment and the first experiment

According to the theory proposed by Thomas that the heat release or absorption of gas is proportional to the mass flow[17], gas flow can be measured indirectly by obtaining temperature change from the FBG sensor. Therefore, the inlet flow changes can accurately reflect the temperature field distribution on the cylinder.

We took cardboard cylinder as the inlet of diesel engine and used adjustable air blower and aerovane as gas source. The thermoelectric bridge balance was utilized to maintain the FBG sensor at 127 °C in order to eliminate the measurement temperature difference caused by the outside air temperature[18]. The FBG probe was fastened on the inlet port wall. Firstly, we varied the wind velocity forward from 1.5 m/s to 5.0 m/s gradually, and recorded the fiber grating center wavelength under different wind speeds. Secondly, we decreased the wind velocity backward from 5.0 m/s to 1.5 m/s, and recorded the center wavelength simultaneously. The center wavelength is 1 550.072 nm at room temperature of 27 °C.

Fig.10 depicts the fiber grating center wavelength shift curves caused by change of velocity based on the forward and backward experiments. It's evidenced that the center wavelength of FBG shifts with the change of velocity, and the shift center wavelength is linearly proportional to the wind velocity.

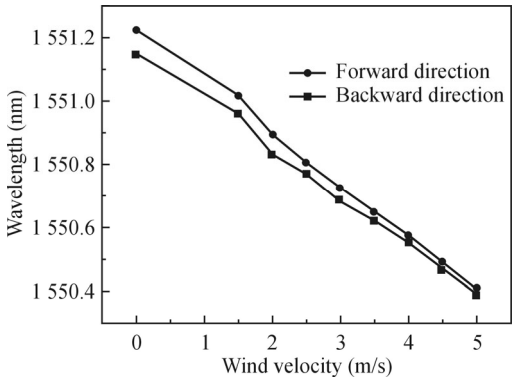

Fig.10 The center wavelength shift versus the change of the wind velocity

In our experiment, the gas is considered as ideal gas. According to Charlie's law, the volume flow under the standard condition can be obtained approximately. Through the cross-sectional area S of cardboard cylinder and wind velocity v obtained by aerovane, the volume flow can be given by

$$V = \int_0^t Sv \,, \tag{4}$$

where t is the ventilation time. Because the conversion relation between volume flow V and mass flow W is $W=\rho V$, where ρ is the density of gas, the mass flow can be further procured by

$$W = \rho \int_0^t Sv \,. \tag{5}$$

Through the above relationship, we can not only obtain the average temperature of measurement point on cylinder head, but also acquire the intrinsic relationship between the center wavelength of FBG and gas flow. The gas flow test provides a new method for discussing the thermal load of cylinder head in diesel engine.

In this paper, a novel optical fiber based technique for monitoring the temperature of cylinder head and the gas flow of diesel engine is proposed. The FBG temperature probe within capillary tube is investigated and produced. The distribution of temperature field on cylinder head is simulated, and the simulation results agree well with the experimental results. The research results demonstrate that FBG temperature probe has good repeatability and sensitivity compared with traditional probe. Gas flow simulation implies that the FBG center wavelength shift has a linear relationship with air flow velocity. Our results provide a useful guideline in the investigation of thermal loading of engine cylinder head and open a new avenue for the research of the thermal loading of diesel engine.

References

[1] L. Y. Bian, Mechanical and Electronic **3**, 116 (2011). (in Chinese)

[2] Rakopoulos C. D. and Mavropoulos G. C., Energy Conversion and Management **41**, 1265 (2000).

[3] P. Wang, H. Zhao, Y. G. Man, X. He, Y. T. Sun and J. Liu, Proceedings of the CSEE **32**, 131 (2012).

[4] J. Zubia, C. Vázquez and J. Mateo, Spienewsroom **1117**, 10 (2014).

[5] M. Yang, Z. Chen, K. He and L. Yi, Research on the Health Monitoring Technology of Solid Rocket Motor Based on Embedded Optical Fiber Sensor, Defense Industry Test and Measurement Technology Development Strategy Forum, 2014.

[6] X. J. Fan, Q. Jiang, G. X. Li, Y. P. Hu, Q. L. Wu and Y. Wang, Journal of Testing and Evaluation **43**, 758 (2014).

[7] J. N. Feng, F. J. Duan, D. C. Ye, X. J. Jin and J. N. Zheng, Nanotechnology and Precision Engineering **14**, 167 (2016). (in Chinese)

[8] R. T. Ghahrizjani, H. Sadeghi and A. Mazaheri, IEEE Sensors Journal **16**, 3551 (2016).

[9] Q. Jiang, D. B. Hu and M. Yang, Sensors and Actuators, A: Physical **17**, 62 (2009).

[10] Lan Ruo-ming and Cao Yu-qiang, Optoelectronics Letters **11**, 229 (2015).

[11] Jiang Shan-chao, Wang Jing, Sui Qing-mei and Cao Yu-qiang, Optoelectronics Letters **11**, 81 (2015).

[12] Z. C. Yang, Fabrication and Study of High-Temperature Resistant Fiber Gratings, China Jiliang University, 2012. (in Chinese)

[13] G. Yang, C. Leitão, Y. Li, J. Pinto and X. Jiang, Measurement **46**, 3166 (2013).

[14] G. X. Li, S. Fu, Y. Liu, S. Z. Bai and L. Cheng, , Energy Conversion and Management **50**, 1862 (2009).

[15] Yu Xiu-Juan, Yu You-long, Zhang Min, Liao Yan-biao and Lai Shu-rong, Journal of Optoelectronics·Laser **17**, 564 (2006). (in Chinese)

[16] G. P. Zhou, Piezoelectrics & Acoustooptics **32**, 534 (2010). (in Chinese)

[17] K. G. Wu, Journal of Chang'an University Natural Science Edition) **22**, 86 (2002). (in Chinese)

[18] P. L. Su, Vehicle Repair and Maintenance **7**, 38 (2001). (in Chinese)